Journal of Peptide Science
J. Peptide Sci. **5**: 507–518 (1999)

Structure Investigation of Amphiphilic Cyclopeptides in Isotropic and Anisotropic Environments—A Model Study Simulating Peptide–Membrane Interactions

MARCUS KOPPITZ, BARBARA MATHÄ and HORST KESSLER*

Institute of Organic Chemistry and Biochemistry, Technische Universität München, Garching, Germany

Received 8 May 1999
Accepted 12 May 1999

Abstract: It has been proposed that the membrane allows a much more efficient binding of certain small or medium-sized amphiphilic messenger molecules to their receptor, not only by accumulation of the drug, but also by induction of orientations and conformations that are much more favorable for receptor docking than structures adopted in isotropic phases. A series of eight amphiphilic cyclic peptides containing lipophilic (L-α-aminodecanoic acid = Ada, L-α-aminohexadecanoic acid = Ahd, Nhdg = *N*-hexadecylglycine) and hydrophilic (Lys, Asp) amino acids were synthesized and examined by means of NMR spectroscopy and molecular dynamics (MD) simulations in isotropic ($CDCl_3$) and membrane-mimicking anisotropic (SDS/H_2O) solvents to study the influence of the environment on their individual conformations. NMR data of *cyclo*(-Gly^1-D-Asp^2-Ahd^3-Ahd^4-Asp^5-Gly^6-) (**C4**), *cyclo*(-Lys^1-D-Pro^2-Lys^3-Ada^4-Pro^5-Ada^6-) (**C5**) and *cyclo*-(-Lys^1-Pro^2-Lys^3-Ada^4-D-Pro^5-Ada^6-) (**C6**) clearly indicate that those compounds are too rigid to perform a conformational change upon transition from an isotropic to an anisotropic environment. On the other hand, the experimental data of *cyclo*(-Gly^1-Asp^2-Ahd^3-Ahd^4-Asp^5-Gly^6-) (**C1**), *cyclo*(-Asp^1-Ala^2-Nhdg^3-Ala^4-D-Asp^5-) (**C7**), and *cyclo*(-D-Asp^1-Ala^2-Nhdg^3-Ala^4-Asp^5-) (**C8**) suggest highly flexible unstructured molecules in both environments. However, for *cyclo*(-Asp^1-Asp^2-Gly^3-Ahd^4-Ahd^5-Gly^6-) (**C2**) we observed **a structure inducing effect** of a membrane-like environment. The compound populates three different conformations in SDS/H_2O, whereas in $CDCl_3$ no preferred conformation can be detected. *cyclo*(-D-Asp^1-Asp^2-Gly^3-Ahd^4-Ahd^5-Gly^6-) (**C3**) clearly exhibits **two different conformations** with a shifted β,β-turn motif **in $CDCl_3$ and SDS/H_2O solutions**. The conformational change could be reproduced in a restraint-free MD simulation using the biphasic membrane mimetic CCl_4/H_2O. Our results give clear evidence that membrane interactions may not only lead to structure inductions, but can also induce major conformational changes in compounds already exhibiting a defined structure in isotropic solution. Copyright © 1999 European Peptide Society and John Wiley & Sons, Ltd.

Keywords: cyclic peptides; amphiphilic; membranes; structure investigation

INTRODUCTION

The recognition process between certain amphiphilic messenger molecules and their membrane-bound receptors is supposed to be preceded by a pre-adsorption to the membrane of the target cell and subsequent two-dimensional diffusion to the receptor [1–3]. In the first step, the drug is adsorbed to the membrane by mainly hydrophobic, but also electrostatic interactions. In the second step, two-dimensional diffusion in the membrane finally allows docking to the specific receptor. Functions attributed to the membrane include the increase of the effective concentration, a pre-orientation for the binding to the receptor and the induction of conformations favorable for receptor binding. This model was originally developed for linear opioid peptides [4]. Linear compounds in general exhibit no defined conformation in isotropic

* Correspondence to: Institute of Organic Chemistry and Biochemistry, Technische Universität München, Lichtenbergstr. 4, D-85747 Garching, Germany. E-mail: kessler@ch.tum.de

CCC 1075–2617/99/110507-12$17.50

environments like water, but often adopt a more defined secondary structure like an amphiphilic α-helix or a β-sheet when bound to the membrane [5–12]. However, other compounds are also known to interact with membranes that lack these 'classical' structural motifs. These biological messenger molecules, like for example mating factors of the lower eucariotic organisms yeast and fungus [13,14] or cytostatic acting peptides found in algae [15], usually achieve hydrophobic interactions by attachment of lipophilic anchors at cysteins, threonines [16] or at the *N*-terminus. Incorporation of unnatural lipophilic amino acids is also observed [17,18]. A higher concentration at the membrane interphase seems to be the main purpose of the lipophilic modification of proteins (see e.g. for ras [19]). Some examples are also reported that give evidence for the induction of a distinct conformation or for a change of the three-dimensional structure in membrane-like environments [20–26].

It is the purpose of this study to design small model peptides with defined lipophilic and hydrophilic regions, in order to investigate if interactions with membrane-like environments can lead to structure-inductions or even conformational changes in simple model compounds. We have chosen cyclic peptides because their reduced conformational space allows a more accurate and precise determination of their three-dimensional space than in linear and very flexible peptides.

MATERIALS AND METHODS

Peptide Synthesis

All peptides were assembled manually on a 2-chlorotritylchloride resin applying Fmoc-based SPPS. Fmoc-Ahd-OH (Ahd = L-α-aminohexadecanoic acid), Fmoc-Ada-OH (Ada = L-α-aminodecanoic acid) and Fmoc-Nhdg-OH (Nhdg = *N*-hexadecylglycine) were obtained as previously described [61]. Loading of the resin with 1 mmol amino acid/g resin was achieved using 1.1 mmol of Fmoc-Asp(*t*Bu)-OH (Asp^1 for **C7**, Asp^2 for **C2** and **C3**, Asp^5 for **C1**, **C4** and **C8**), Fmoc-Pro-OH (Pro^5 for **C5**) or Fmoc-D-Pro-OH (D-Pro^5 for **C6**) according to the published procedure [27]. Synthesis was carried out using 2.5 equivalents of Fmoc-Xxx-OH/TBTU/HOBt and DIPEA in NMP for coupling and 20% piperidine in DMF for cleavage of the Fmoc moiety. Treatment of the resin with HOAc:TFE:DCM (1:1:3) for 1 h and removal of the solvent yielded the side-chain protected linear peptide acids [28]. Addition of 3 equivalents of DPPA and 5 equivalents of solid $NaHCO_3$ and stirring for 24 h gave the crude cyclic peptides after filtration, evaporation of the solvent and washing with water [29,30]. Purification of the side-chain protected cyclopeptides was achieved by flash-chromatography [31] in $CDCl_3$/MeOH (19:1) yielding > 98% homogeneous material. For side-chain deprotection, the peptides were treated for 30 min with 50% TFA in DCM at room temperature. Overall yields were 79% (**C1**), 58% (**C2**), 70% (**C3**), 77% (**C4**), 65% (**C5**), 62% (**C6**), 49% (**C7**) and 47% (**C8**) referring to resin-bound peptide. The obtained, completely deprotected peptides, readily form aggregates and therefore cannot be analyzed or purified by RP-HPLC on C18 columns. All protected and deprotected cyclopeptides were characterized by FAB-MS and NMR spectroscopy.

NMR Spectroscopy

All NMR spectra were recorded on Bruker AMX 600, AMX 500 and AC 250 spectrometers and processed on an Aspect X32 station with the UXNMR software package (Bruker). The measurements were performed at 300 K using 0.9–2 mM solutions of the peptides in H_2O/10% D_2O, $CDCl_3$ or DMSO-d_6 and 4 mM solutions of the peptides in a 320 mM solution of SDS in H_2O/10% D_2O. All chemical shifts are referenced to the solvent signal ($CDCl_3$: 7.24 ppm (^{1}H) and 77 ppm (^{13}C); DMSO-d_6: 2.49 ppm (^{1}H) and 38.5 ppm (^{13}C)) or to the signal of added TSP at 0 ppm (^{1}H) and 0 ppm (^{13}C) for measurements in H_2O or SDS/H_2O. Assignment of resonances was achieved by 2D-NMR techniques (TOCSY [32,33], NOESY [34], ROESY [35–37], HMQC [38,39], HMQC-TOCSY [40,41]) applying presaturation or jump return [42] for suppression of the solvent in SDS/water mixtures. Mixing times were 20 and 80 ms for TOCSY spectra, 120 ms for NOESY or ROESY spectra in isotropic solvent and 40 ms for NOESY spectra in SDS/H_2O. Quantitative information on interproton distances for the structure investigation was obtained by analyzing NOESY and ROESY spectra using the isolated two-spin approximation [43] (ISPA) and a correction for the jump return excitation profile. Deuterium exchange reactions in $CDCl_3$ were performed by shaking with 100 µL D_2O, which was added to the respective sample. Deuterium exchange in SDS solution was performed by dissolving peptide and SDS in pure D_2O.

Computer Simulations

The peptides **C2**, **C3** and **C1** were analyzed using either distance geometry (DG) or simulated annealing (SA) calculations. If convergence in one of these methods was obtained, a molecular dynamics (MD) calculation in explicit solvent was performed.

The structure calculations were carried out on Silicon Graphics Indy™ R4600 and SP2 computers. DG calculations were carried out using a modified version of DISGEO [45–48]. The DG procedure started with the embedding of 100 structures using random metrization [49]. For the refinement of the structures, DISGEO employs distance- and angle-driven dynamics with the NOE-restraints and an additional harmonic ^3J-coupling potential [44] according to the Karplus equation. From the resulting 100 structures, the 10–20 low error structures were examined. If convergence is achieved, an additional DG calculation is performed including floating chiralities [80] to determine the diasterotopic assignment of the glycine H$^{\alpha}$s.

In addition, SA calculations [50] were carried out for all three peptides. The basis of SA involves a randomization of the coordinates, minimization and MD calculation at 1000 K for 5 ps, followed by a cooling order to overcome the local minima. In the cooling phase the temperature was lowered in 50.0 K steps of 1 ps dynamics to 300.0 K. The resulting structure was then minimized using the steepest descent and conjugate gradient. During the whole calculation period, the NOE-constraints were incorporated with a force constant of 10.0 kcal/A^2 mol and the homonuclear coupling constants were included as harmonic potential according to the Karplus equation. Additionally, the chiralities were fixed and the peptide bonds were set to *trans*; 100 structures were generated. The resulting structures were analyzed due to their convergence. If convergence is obtained, an additional MD calculation is carried out in explicit solvent.

The MD calculations were carried out with the program DISCOVER 95.0 using the CVFF89 forcefield [51,52]. In the case of $CDCl_3$ as solvent used in NMR investigations, the resulting low error or low energy structures from DG or SA calculations, were placed in a cubic box and soaked with $CHCl_3$ including periodic boundary conditions. For SDS/H_2O solutions, the peptide was placed into the two-phase H_2O/CCl_4 [73] simulation cell using three-dimensional periodic boundary conditions. The peptide was positioned at the phase interface with the alkylchain of the Ahd[4] and Ahd[5] residues embedded in the apolar phase. The two-phase box has been shown to be a powerful membrane-mimic [74], which reduces the anisotropic environment to two solvents of differing polarity, viscosity, and H-bonding capabilities.

During all the MD calculations a time step of 1 fs was employed. The minimization steps were separated in two cycles of conjugate gradient energy minimization. In the first step, the solute was fixed and then all atoms were allowed to remove freely. Then the system was heated gradually in 50.0 K steps from 50.0 to 300 K in 2 ps steps, each by direct velocity scaling. After an equilibration period with temperature coupling of 20 ps for the isotropic environment or 50 ps for the anisotropic environment, respectively, the configurations were saved every 200 fs for another 100 ps. During the simulations, the distance restraints were included as well as the homonuclear ^3J-coupling constants as harmonic potentials according to the Karplus equation. The MD simulations were continued without restraints for another 50 ps with the sampling rate unchanged.

An additional simulation in the two-phase box was performed with the averaged and energy-minimized conformation of **C3** resulting from restraint MD in $CHCl_3$ embedded completely in the apolar phase. The aspartic acid side chains were treated as charged with Na^+ as counterions. The neighbor lists for calculation of non-bonded interactions were updated every 10 fs within a radius of 14 Å, and the actual calculation of the non-bonded interactions was carried out up to a radius of 12 Å. The simulations protocol is the same as in the procedure described above.

APPROACH

An important requirement for the design of our amphiphilic model peptides was conformational control. Since linear compounds, at least in isotropic environments, often exhibit random coil structures, we decided to use cyclic penta- and hexapeptides [53] obtained by head-to-tail cyclization. Their conformational behavior in isotropic solution is known from numerous and extensive NMR studies over previous decades. Furthermore, the envisaged peptides should exhibit defined hydrophilic and lipophilic regions within the molecule, which would allow a specific and sufficiently strong interaction with the model membrane. Investigation of cyclic hexapeptides where leucine was

incorporated as a hydrophobic amino acid, demonstrated that natural amino acids could not introduce enough hydrophobicity into these small molecules for a significant interaction with micelles [54]. This is in agreement with studies on membrane-active, lipid-modified messenger molecules, where it has been shown that a minimum length of the lipid anchor is essential for their biological activity [55–59].

We therefore synthesized and incorporated unnatural lipophilic long chain α-amino acids L-α-aminodecanoic acid (Ada) and L-α-aminohexadecanoic acid [60] (Ahd) or the *N*-alkylated *N*-hexadecylglycine (Nhdg) into the hydrophobic region. The hydrophilic part was generated by lysine or aspartic acid. The remaining positions were filled up with proline, alanine or glycine. Proline was chosen because it strongly induces distinct conformations and *cis*/*trans* isomers of the adjacent amide bond are of similar energy. As those conformations are slowly interconverting on the NMR timescale, conformational changes induced by the environment can be easily observed directly. Alanine or glycine was only used as a separator between hydrophilic and hydrophobic regions. On the other hand, glycine lacks a side chain at the α-carbon that allows more flexibility and may act for example as a L- or D-amino acid. Therefore, several energetically similar conformations were to be expected, in which conformational changes in different environments could be observed. This finally led to the design of the following cyclic peptides:

cyclo(-Gly^1-Asp^2-Ahd^3-Ahd^4-Asp^5-Gly^6-) (**C1**),
cyclo(-Asp^1-Asp^2-Gly^3-Ahd^4-Ahd^5-Gly^6-) (**C2**),
cyclo(-D-Asp^1-Asp^2-Gly^3-Ahd^4-Ahd^5-Gly^6-) (**C3**),
cyclo(-Gly^1-D-Asp^2-Ahd^3-Ahd^4-Asp^5-Gly^6-) (**C4**),
cyclo(-Lys^1-D-Pro^2-Lys^3-Ada^4-Pro^5-Ada^6-) (**C5**),
cyclo(-Lys^1-Pro^2-Lys^3-Ada^4-D-Pro^5-Ada^6-) (**C6**),
cyclo(-Asp^1-Ala^2-Nhdg^3-Ala^4-D-Asp^5-) (**C7**),
cyclo(-D-Asp^1-Ala^2-Nhdg^3-Ala^4-Asp^5-) (**C8**).

D-Residues in cyclic peptides are known to induce distinct conformations and are often found in the $i+1$ position of a βII′ turn. Hence, the competition of their conformational influence with that of glycine and/or proline led us to expect conditions for the observation of conformational changes by environmental influences.

RESULTS

General

The conformations of these peptides were determined by NMR spectroscopy (temperature gradients of the amide protons, deuterium exchange rates, $^3J(H^N–H^\alpha)$ coupling constants, and NOE-derived interproton distances). In addition DG and MD calculations were performed. For the NMR studies in anisotropic environment, SDS/H_2O solution was chosen, which has proven to be a mimetic for membranes [61–64]. For some peptides a structure investigation was not possible in pure water (isotropic environment) because of spontaneous formation of aggregates even at the lowest concentrations. We then used $CHCl_3$ as the isotropic solvent, which should simulate the lipophilic core of a membrane. In addition, the resulting structure could also be used as an initial structure for subsequent free MD simulations in our membrane-mimicking biphasic system (see below). However, concentration dependent aggregation phenomena were also observed in this solvent (cf. Figure 1), and consequently, highly dilute solutions had to be used. Due to the insolubility of the peptides **C1**, **C2** and **C3** with free carboxyl side chains at the aspartic acids, we investigated their *t*-Bu esters in $CDCl_3$.The MD simulations were performed in explicit solvents [65–71] to prevent vacuum artifacts [72]. For the measurements in SDS/H_2O we utilized a CCl_4/H_2O two-phase system as a membrane mimetic [73], which compared with a real membrane reduces the number of atoms in a simulation by several orders of magnitude. This system also allows a simulation of the penetration and orientation process at the interphase and has been shown to reproduce structure inductions caused by membrane-like environments [74,75].

Rigid Backbones

C4 in SDS/H_2O and DMSO. The backbone of **C4** shows no evidence for a conformational change upon transition from an isotropic to an anisotropic environment (data not shown). **C4** exhibits the classical β,β-motif with Asp^2 in the $i+1$-position of a βII′-turn in both of the solvents used, SDS/H_2O and DMSO. The compound forms aggregates in H_2O and in $CDCl_3$ which prevent a detailed investigation in these solvents.

C5 and C6 in H_2O and SDS/H_2O. **C5** and **C6** are derivatives of *cyclo*(-Phe-D-Pro-Phe-Phe-Pro-Phe-), which has been shown to exhibit an equilibrium between a *trans*/*trans* βII/βII- and a *cis*/*trans* $\beta VI_a/\gamma$-conformation [76]. However, we observed more than 95% of the *trans*/*trans*-arrangement in both solvent systems H_2O and SDS/H_2O (data not shown).

Flexible backbones

C1 in $CDCl_3$ and SDS/H_2O. **C1** is an all-L-compound with two sequential glycines, that might favor a potential conformation with Gly^1 in the $i+1$-position of a βII′-turn (Gly as a mimic for a D-amino acid). However, the NMR-derived structure parameters in $CDCl_3$ and SDS/H_2O do not indicate a preference for a distinct β,β-arrangement (cf. Tables 1 and 2). In accordance with this, neither DG nor SA calculations performed for **C1** with the NMR data from $CDCl_3$ and SDS micelles resulted in a preferred conformation. Because no unbiased structure from DG and SA calculations could be obtained, we did not perform a subsequent MD refinement in explicit solvents.

C7 and C8 in $CDCl_3$ and SDS/H_2O. Similarly, the backbone of the cyclic pentapeptides **C7** and **C8** is too flexible to allow the assignment of a defined conformation. The data not only indicate no preference for a certain structure, but in addition are very similar in both $CDCl_3$ and SDS/H_2O (data not shown).

Semi-Rigid Backbones

C2 in $CHCl_3$. This all-L-peptide contains two glycines separated by two amino acids and, therefore, might potentially adopt a β,β-motif with the glycines in the $i+1$-position of each turn. The obtained temperature gradients (Gly^3 15 ppb/K in $CDCl_3$) and deuterium

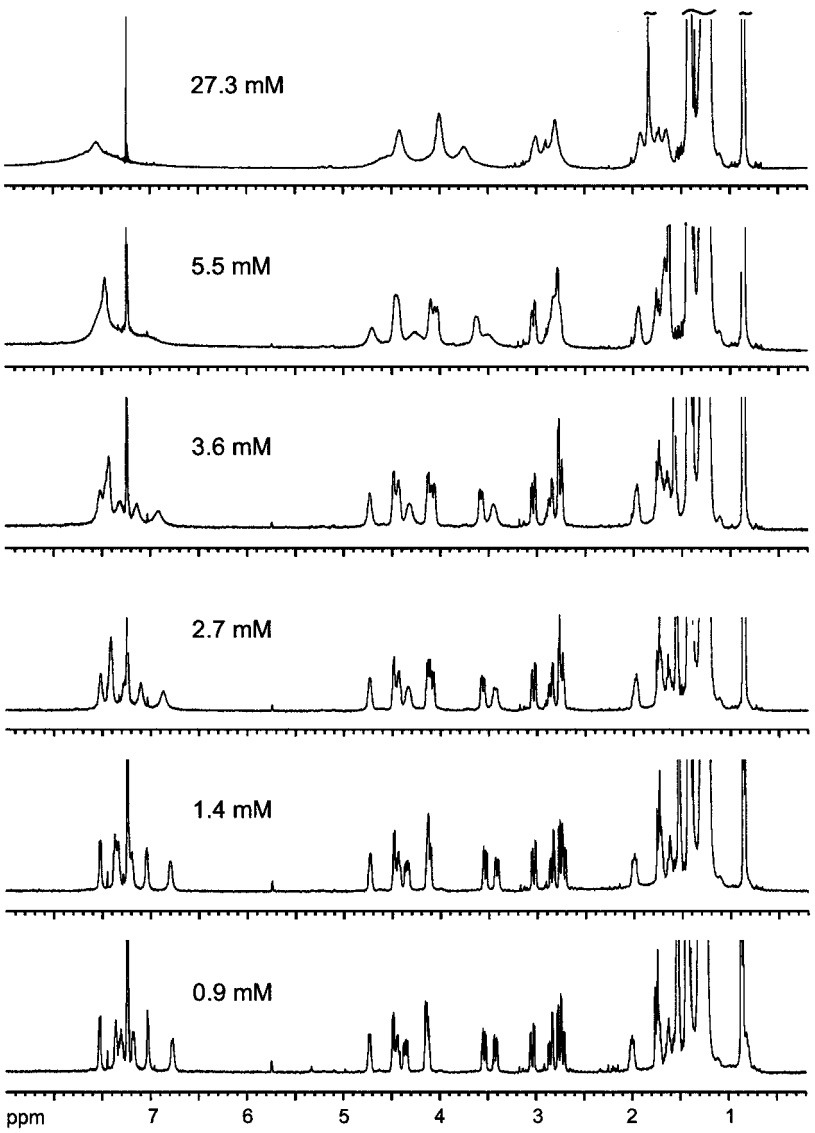

Figure 1 Concentration-dependent ^{1}H-NMR spectra of *cyclo*(-Asp^1-Asp^2-Gly^3-Ahd^4-Ahd^5-Gly^6-) (**C2**) in $CDCl_3$ at 300 K.

Table 1 Chemical Shift Data, Temperature Dependence and Deuterium Exchange Rates of the Amide Protons, and $^3J(H^N–H^\alpha)$ Vicinal Coupling Constants of **C1**, **C2** and **C3** in $CDCl_3$ and SDS/H_2O

C1	Solvent	Gly[1]	Asp[2]	Ahd[3]	Ahd[4]	Asp[5]	Gly[6]
$\delta(H^N)$	$CDCl_3$	6.80	7.02	7.25	6.49	7.34	7.49
[ppm]	SDS/H_2O	8.03	8.56	8.21	7.74	8.56	8.56
$\Delta\delta/\Delta T$	$CDCl_3$	1.4	3.0	2.3	−1.0	2.3	1.7
[−ppb/K]	SDS/H_2O	−9.1	−4.6	−6.3	−9.0	−4.6	−6.8
D_2O-exchange	$CDCl_3$	<18 h	>18 h	>18 h	>18 h	>18 h	<5h
	SDS/H_2O						
$^3J(H^N–H^\alpha)$	$CDCl_3$	7.8/5.0	9.7	7.1	5.5	8.9	
[Hz]	SDS/H_2O						

C2	Solvent	Asp[1]	Asp[2]	Gly[3]	Ahd[4]	Ahd[5]	Gly[6]
$\delta(H^N)$	$CDCl_3$	7.53	7.17	7.36	7.02	6.76	7.30
[ppm]	SDS/H_2O	8.53	8.36	7.76	8.39	7.84	7.92
$\Delta\delta/\Delta T$	$CDCl_3$	2.9	7.3	15.1	8.4	6.5	6.7
[−ppb/K]	SDS/H_2O	4.6	3.3	5.3	7.7	4.6	5.3
D_2O-exchange	$CDCl_3$	<5 h	>8 days	<8 days	>8 days	>8 days	<18 h
	SDS/H_2O						
$^3J(H^N–H^\alpha)$	$CDCl_3$	7.0	9.2	5.4/7.5	7.0	8.9	
[Hz]	SDS/H_2O		9.0			8.9	

C3	Solvent	D-Asp[1]	Asp[2]	Gly[3]	Ahd[4]	Ahd[5]	Gly[6]
$\delta(H^N)$	$CDCl_3$	6.80	7.06	7.37	6.47	7.16	7.35
[ppm]	SDS/H_2O	8.59	8.70	8.07	8.39	8.02	7.56
$\Delta\delta/\Delta T$	$CDCl_3$	5.7	5.0	4.4	8.0	3.6	2.3
[−ppb/K]	SDS/H_2O	7.0	7.0	5.3	6.7	5.3	3.0
D_2O-exchange	$CDCl_3$	<6 h	>7 days	<48 h	<7 days	>7 days	<48 h
	SDS/H_2O	<3 min	<3 min	>3 min	<3 min	<3 min	<3 min
$^3J(H^N–H^\alpha)$	$CDCl_3$	8.5	8.9		6.3	8.2	
[Hz]	SDS/H_2O		9.0			8.7	

exchange rates (together with Asp[1] fastest exchange rates for both glycines) indeed support this idea (cf. Table 1). However, the subsequent DG calculation did not lead to a converging structure, which can be attributed to either a lack of sufficient experimental data or to a high conformational flexibility. Also, SA calculations, which include forcefield information, did not result in a converging low energy structure. When taking a closer look at the distances, this result is not astonishing (cf. Table 3) as all obtained NOE-derived interproton distances range between 240 and 310 pm. Obviously, **C2** does not adopt a preferred conformation in $CDCl_3$.

C2 in SDS/H₂O. The interproton distances obtained in micellar solution show a higher dispersion and deviate significantly from the distances in $CDCl_3$ (cf. Table 3). A manual analysis of the obtained data might finally suggest a conformation with the glycines in the i and $i+4$-positions of a β-turn. On the other hand, a DG calculation did not result in a single converging structure. Three structural families can be identified out of the ten structures with the lowest energy obtained from SA calculations. One family consists of four structures (RMSD < 0.2 Å) and exhibits a γ-turn between Ahd[5] and Asp[1] (Plate 1a). The overall conformation resembles a β-turn motif with Gly[3] and Gly[6] in the $i+1$ position. The second family consists of three structures, with Asp[1] and Ahd[4] in the $i+1$ position of a β-turn like motif (Plate 1b). The remaining three structures are represented by Plate 1c. As in family 1 the glycines are in the $i+1$-position of a β-turn-like motif.

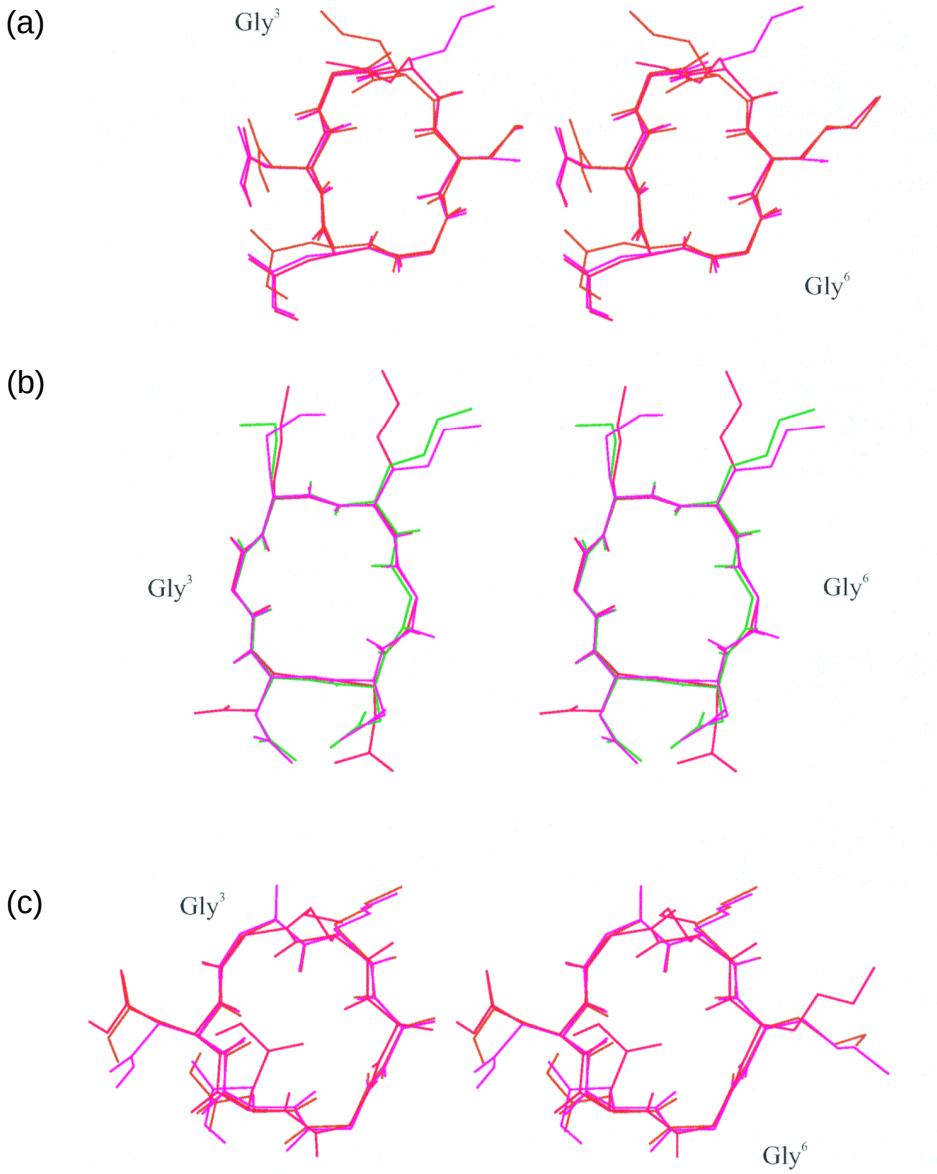

Plate 1 Stereoview of family 1(a), family 2(b) and family 3(c) of ***C2*** in SDS micelles resulting from Simulated Annealing. For clarity, the length of the side chains has been restricted to four C-atoms.

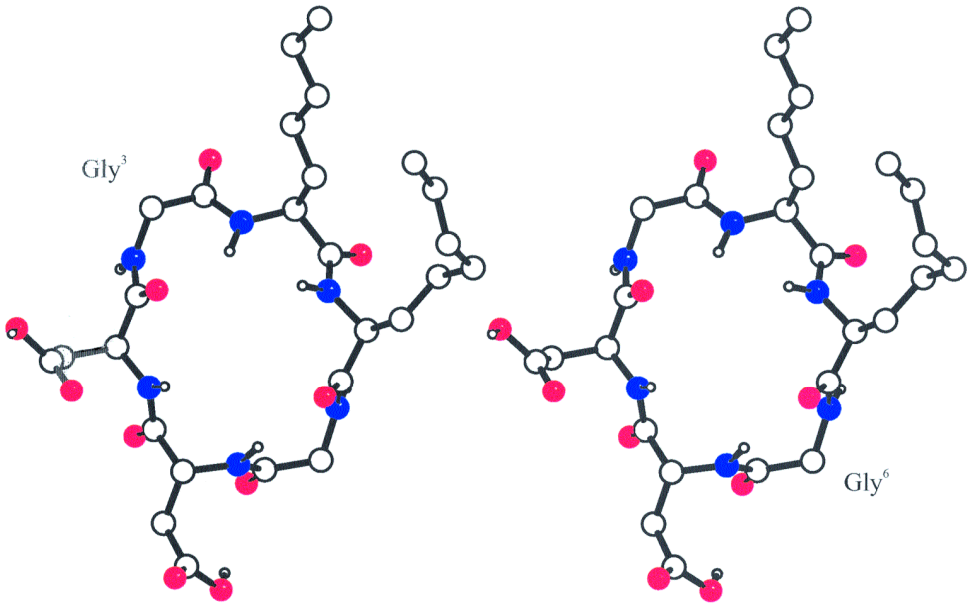

Plate 2 Stereopicture of the averaged and energy-minimized structure of 100 ps rMD of ***C3*** in $CHCl_3$.

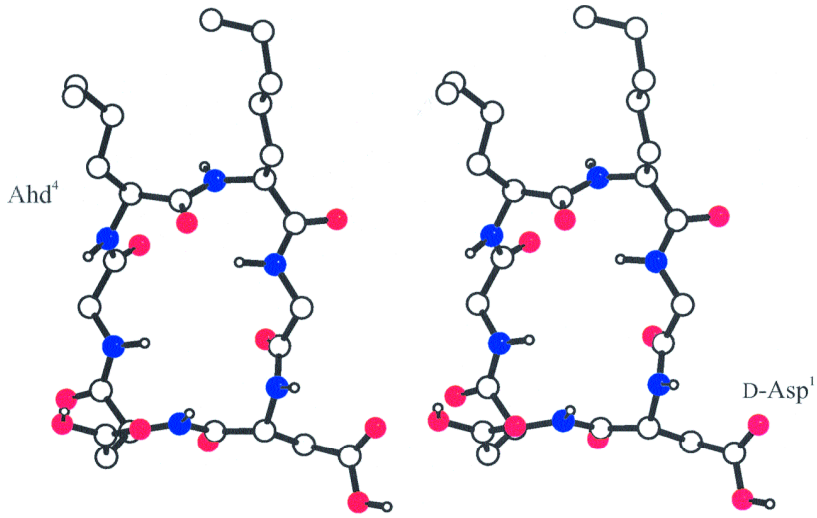

Plate 3 Stereopair of the averaged and energy-minimized structure of 100 ps rMD of ***C3*** in H_2O/CCl_4.

The NOE-violations of each individual family are high. However, all ten conformations taken together agree reasonably well with the NMR data. This indicates that more than one conformation is populated in SDS micelles. Due to the difficulties in obtaining a sufficient number of NMR parameters with good quality, no ensemble DG calculation [77–79] was performed.

C3 in $CHCl_3$. **C3** is the epimer of **C2** (D-Asp^1 instead of L-Asp^1 in **C2**). This should enhance the competition of Asp^1 with the glycines for the $i+1$-position of a β-turn and also lead to a reduced flexibility. The obtained NMR data indeed suggest the formation of a defined structure (cf. Table 1). For example, the deuterium exchange experiment clearly reveals the fastest exchange rate for D-Asp^1, followed by the glycines and Ahd^4, which might be indicative of a hydrogen bond between Asp^2 and Ahd^5 and therefore would place the glycines in the $i+1$-position of a potential β-turn. Moreover, in contrast to **C2**, the obtained interproton distances display a significant dispersion, thereby underlining the presence of a preferred conformation. We subsequently performed DG calculations with 23 NOESY derived distances and four $^3J(H^N–H^\alpha)$ coupling constants. Since the low energy structures converged, the glycine H^αs were assigned diastereotopically using floating chiralities [80]. The conformation with the smallest total error was chosen for a subsequent restraint MD calculation in explicit $CHCl_3$. After equilibration, the resulting average structure from 100 ps restrained MD is displayed in Plate 2. The effective distances between atoms involved in NOEs were determined by calculating the inverse cube of the distance, r^{-3}, for each configuration and then averaging this value over the trajectory [81]. **C3** clearly prefers a β,β-turn motif in $CHCl_3$ with both glycines in an $i+1$ position. Ideal β-turns, however, are not formed.

Table 2 Comparison of Interproton Distances of **C1** Derived from NOESY Experiments in $CDCl_3$ and SDS/H_2O

C1 Distance	$CDCl_3$ d_{NOE} [pm]	SDS/H_2O d_{NOE} [pm]
$Gly^1H^N–Asp^2H^N$	260	
$Gly^1H^N–Gly^6H^N$		290
$Asp^2H^N–Ahd^3H^N$		260
$Ahd^3H^N–Ahd^4H^N$		260
$Ahd^4H^N–Asp^5H^N$	250	
$Gly^1H^N–Gly^6H^{\alpha h}$	370	270
$Gly^1H^N–Gly^6H^{\alpha t}$		270
$Gly^6H^N–Gly^6H^{\alpha h}$	280	215
$Gly^6H^N–Gly^6H^{\alpha t}$	340	260
$Gly^6H^N–Asp^5H^\alpha$	280	overlap
$Asp^5H^N–Asp^5H^\alpha$	300	overlap
$Asp^5H^N–Ahd^4H^\alpha$	380	overlap
$Ahd^4H^N–Ahd^4H^\alpha$	380	250
$Ahd^4H^N–Ahd^3H^\alpha$	400	310
$Ahd^3H^N–Ahd^3H^\alpha$	260	260
$Ahd^3H^N–Asp^2H^\alpha$	260	320
$Asp^2H^N–Asp^2H^\alpha$	310	overlap
$Asp^2H^N–Gly^1H^{\alpha h}$	360	230
$Asp^2H^N–Gly^1H^{\alpha t}$	360	250

Table 3 Comparison of Interproton Distances of **C2** Derived from NOESY Experiments in $CDCl_3$ and SDS/H_2O

C2 Distance	$CDCl_3$ d_{NOE} [pm]	SDS/H_2O d_{NOE} [pm]
$Asp^1H^N–Asp^2H^N$	260	
$Asp^2H^N–Gly^3H^N$		350
$Ahd^4H^N–Ahd^5H^N$	290	340
$Asp^1H^N–Asp^1H^\alpha$	280	300
$Asp^1H^N–Gly^6H^{\alpha h}$	280	300
$Asp^1H^N–Gly^6H^{\alpha t}$	250	240
$Gly^6H^N–Gly^6H^{\alpha h}$	250	290
$Gly^6H^N–Gly^6H^{\alpha t}$	270	320
$Gly^6H^N–Ahd^5H^\alpha$	260	300
$Ahd^5H^N–Ahd^5H^\alpha$	280	290
$Ahd^5H^N–Ahd^4H^\alpha$	290	380
$Ahd^4H^N–Ahd^4H^\alpha$	290	320
$Ahd^4H^N–Gly^3H^{\alpha h}$	310	300
$Ahd^4H^N–Gly^3H^{\alpha t}$	260	250
$Gly^3H^N–Gly^3H^{\alpha h}$	240	290
$Gly^3H^N–Gly^3H^{\alpha t}$	280	350
$Gly^3H^N–Asp^2H^\alpha$	290	330
$Asp^2H^N–Asp^2H^\alpha$	270	270
$Asp^2H^N–Asp^1H^\alpha$	280	380

The measured and calculated interproton distances are given in Table 4. No diastereotopic assignment was possible for Asp^1H^β, Asp^2H^β, Ahd^4H^β, Ahd^5H^β in $CDCl_3$ and for Asp^1H^β, Asp^2H^β, Gly^3H^α, Ahd^4H^β, Ahd^5H^β and Gly^6H^α in SDS/H_2O (cf. Table 4). In these cases, the restraint was assigned to a pseudoatom placed in the middle of the corresponding protons.

The highest restraint violations involve the $Gly^6H^{\alpha(pro\ S)}$ and the D-Asp^1H^N. This could be due to the disturbed β-turn arrangement in this region, because the D-amino acid also favors an $i+1$ position of a β-turn. The calculated coupling constants from 100 ps rMD are in good agreement with the measured coupling constants.

The analysis of the 50 ps free MD-run, which was carried out following the restrained MD calculation, show no major conformational change. This indicates that the structure generated from rMD is energetically favored.

C3 in SDS/H_2O. Both glycines of **C3** exhibit the smallest temperature gradients in micellar solution. The deuterium exchange is very fast, after only 3 min the Gly^3H^N can be detected. Moreover, the only detectable H^N–H^α NOEs are between Asp^2-Gly^3 (290 pm) and Ahd^5-Gly^6 (300 pm) and therefore a structure with glycine in the $i+1$-position, as in $CDCl_3$, appears to be very unlikely. Line-broadening prevented the determination of coupling constants for **C3** in SDS micelles. The DG calculation carried out with 18 NOESY-derived distances gave no meaningful results. Obviously, the number of data is too small. Therefore, SA calculations were performed. Since this calculation procedure results in convergence, the low energy structure was chosen for subsequent MD calculations.

The averaged and energy-minimized conformation from 100 ps rMD of the two-phase simulation is depicted in Plate 3. The measured and calculated interproton distances are given in Table 4. The structure can be characterized by a βII-turn between Gly^6 and Gly^3 and a βI-turn between Gly^3 and Gly^6. This β-turn pattern is in accordance with the low-temperature coefficients for the amide protons of Gly^3H^N and Gly^6H^N (Table 1). However, arguments using the interpretation of the amide temperature coefficient are not very strong, because they might be influenced by the micellar environment. Hydrogen-bonding could be

Table 4 Comparison of Interproton Distances of **C3** Derived from NOESY Experiments in $CDCl_3$ and SDS/H_2O with Distances Obtained from MD Simulations

C3	$CDCl_3$		SDS/H_2O	
Distance	d_{NOE} [pm]	d_{rMD} [pm]	d_{NOE} [pm]	d_{rMD} [pm]
D-Asp^1H^N–Asp^1H^α	292	299	280	257
D-Asp^1H^N–Asp^1H^β	327 [a]	312 [a]	317 [a]	310 [a]
D-Asp^1H^α–D-Asp^1H^β	242 [a]	217 [a]	–	–
D-Asp^1H^N–$Gly^6H^{\alpha(pro\ R)}$	326	352	253 [a]	249 [a]
D-Asp^1H^N–$Gly^6H^{\alpha(pro\ S)}$	370	300	253 [a]	249 [a]
D-Asp^1H^N–Gly^6H^N	369	290	–	–
D-Asp^1H^N–Asp^2H^N	256	321	–	–
Asp^2H^N–Asp^2H^α	292	302	277	309
Asp^2H^N–Asp^2H^β	243 [a]	299 [a]	320 [a]	281
Asp^2H^α–Asp^2H^β	243 [a]	217 [a]	–	–
Asp^2H^N–D-Asp^1H^α	281	234	265	255
Asp^2H^N–Gly^3H^N	–	–	291	305
Gly^3H^N–Asp^2H^α	230	224	290	307
Gly^3H^N–$Gly^3H^{\alpha(pro\ R)}$	336	303	266 [a]	223 [a]
Gly^3H^N–$Gly^3H^{\alpha(pro\ S)}$	227	247	266 [a]	223 [a]
Gly^3H^N–Ahd^4H^N	363	352	–	–
Ahd^4H^N–Ahd^5H^N	294	248	–	–
Ahd^4H^N–$Gly^3H^{\alpha(pro\ R)}$	272	263	243 [a]	251 [a]
Ahd^4H^N–Ahd^4H^α	271	301	243 [a]	251 [a]
Ahd^4H^N–Ahd^4H^β	270 [a]	311 [a]	265 [a]	270 [a]
Ahd^4H^α–Ahd^4H^β	236 [a]	217 [a]	–	–
Ahd^5H^N–Ahd^5H^α	265	301	250	230
Ahd^5H^N–Ahd^4H^α	316	361	–	–
Ahd^5H^N–Ahd^5H^β	268	306 [a]	302 [a]	336 [a]
Ahd^5H^α–Ahd^5H^β	268 [a]	214 [a]	–	–
Gly^6H^N–Ahd^5H^α	238	217	290	315
Gly^6H^N–$Gly^6H^{\alpha(pro\ R)}$	310	294	292 [a]	224 [a]
Gly^6H^N–$Gly^6H^{\alpha(pro\ S)}$	274	243	292 [a]	224 [a]

[a] Distance to pseudoatom.

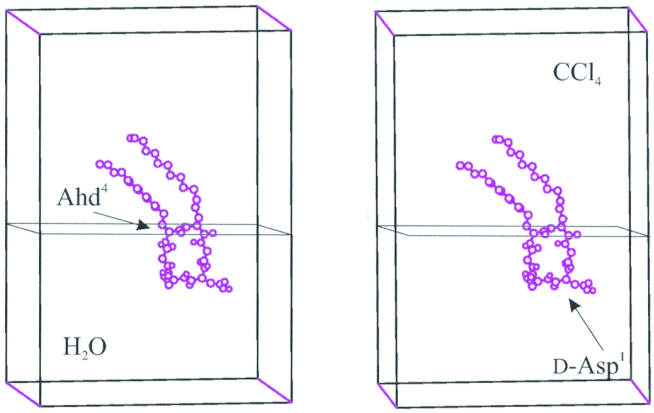

Plate 4 Stereopair of the averaged and energy-minimized structure of ***C3*** obtained by free simulation in the H_2O/CCl_4 2-phase system.

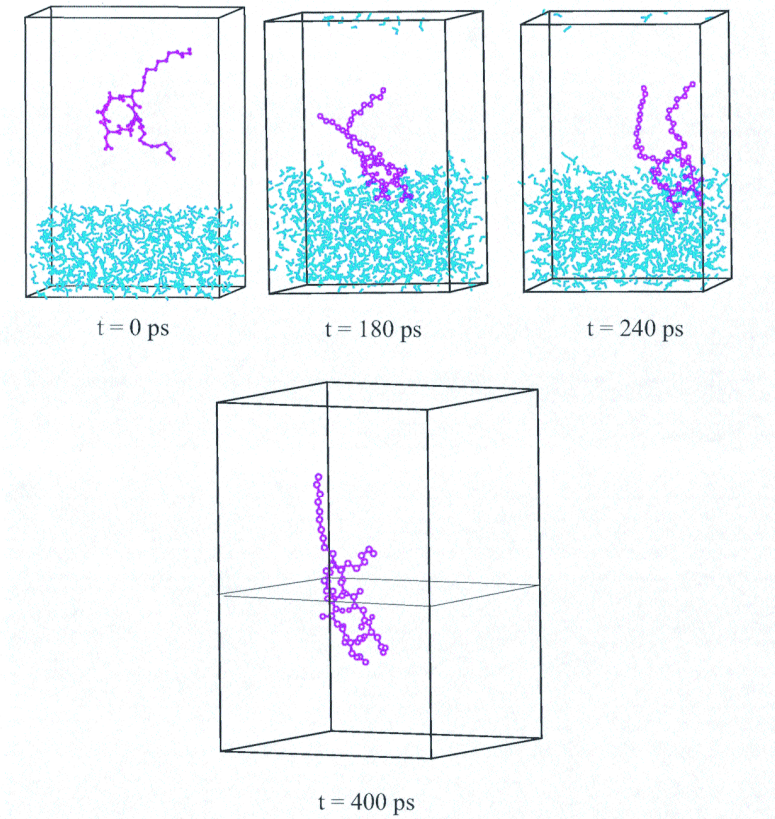

Plate 5 Interdigitation, orientation and conformational change of ***C3*** during the free simulation in the H_2O/CCl_4 2-phase system.

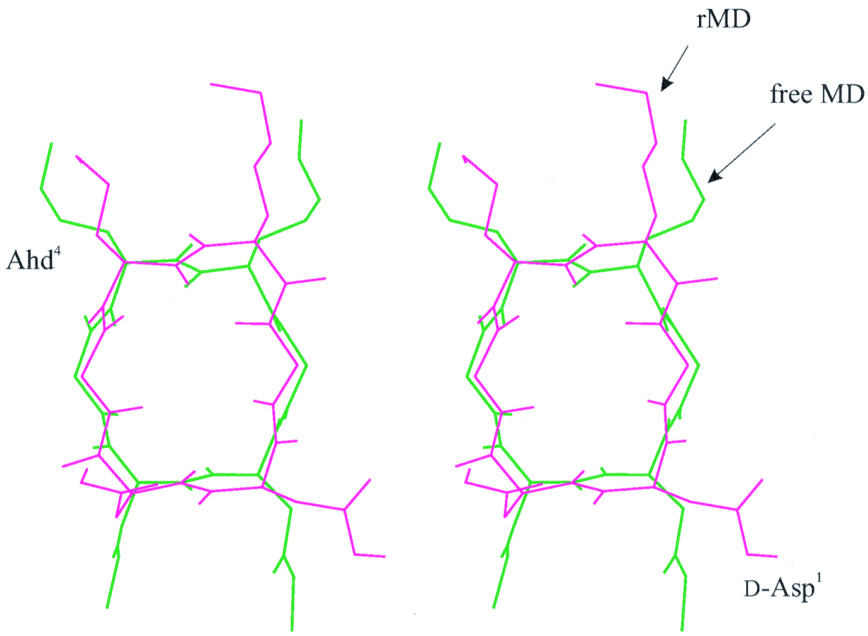

Plate 6 Stereoview of the averaged and energy-minimized conformation of ***C3*** after 100 ps rMD superimposed on the averaged conformation obtained by free simulation in the biphasic H_2O/CCl_4 cell.

observed in the simulation for Gly^6H^N to Ahd^4C^O, which is populated 73% of the simulation time.

The orientation of the molecule in the biphasic environment is displayed in Plate 4. It can clearly be seen that the whole backbone of **C3** is deeply buried in the hydrophilic compartment. Only the two alkyl sidechains of residue Ahd^4 and Ahd^5 are embedded in the lipophilic CCl_4 phase.

The used input distance restraints per se do not allow one to exclude a conformation with the glycines in the $i+1$ position of a β-turn motif. To prove the consistency of the structural data a set of 16 conformations was built up consisting of an ideal β,β-turn pattern with either Gly^3/Gly^6 (eight structures) or D-Asp^1/Ahd^4 (eight structures) in $i+1$-positions. The NOE-violations were calculated for each of these structures. The analysis shows that the structure with the lowest restraint violation forms a βII′-turn between residues Gly^6 and Gly^3 (D-Asp1 in $i+1$) and variable βII or βI-turn motifs between residues Gly^3 and Gly^6 (Ahd^4 in $i+1$). Such a βI, βII equilibrium was often observed in similar cyclic hexapeptides [82]. The artificial structures with the glycines in the $i+1$ position show large NOE-violations, especially the distances between Asp^2H^N and Gly^3H^N and between Gly^6H^N and Ahd^5H^N are violated up to 1 Å (!) in all of the eight conformations. Therefore, we can safely exclude these conformations and assume that D-Asp^1 in the $i+1$-position is strongly favored in SDS micelles.

Free simulation of C3 in a H_2O/CCl_4 two-phase system. The second simulation of **C3** in the two-phase box was performed to confirm, that the conformational switch is indeed induced by a change of the environment, and can be reproduced without application of NMR-derived restraints. We started with the averaged and energy-minimized conformation of **C3** in $CDCl_3$ and embedded the peptide completely into the apolar CCl_4 phase of the two-phase system. We used the sodium salts of the aspartic acid side chains which resulted in a drift towards the aqueous phase that was fast enough to allow observation on the MD time scale. After minimizing the system with the same procedure as in the first calculation, the free simulation was carried out for 500 ps. Plate 5 depicts snapshots of the trajectory of **C3** during the simulation. During the first 200 ps the electrostatic attraction between the charged aspartic acid side chains causes a diffusion of the peptide to the water phase until the whole backbone is completely embedded into the water phase. The $CDCl_3$ conformation is stable until the peptide begins to insert into the water phase. During the interdigitation process, a shift of the β,β-structure occurs and D-Asp^1 is forced into the $i+1$-position of the new β,β-motif. The insertion process can be represented by monitoring the y-coordinates of a certain atom with reference to the H_2O/CCl_4 interphase. Figure 2 illustrates that the C^α of Asp^2 leaves the CCl_4 phase and moves towards the H_2O/CCl_4 interphase region, whereas the C^α of Ahd^4 clearly remains in the CCl_4 phase. The new structure of **C3** does not precisely match the structure obtained by the previous restraint MD calculation in the two-phase system. For example, some deviations can still be observed for the Asp^2H^N–Gly^3H^N interproton distance. However, the resulting overall β,β-motifs of both calculations are identical (Plate 6).

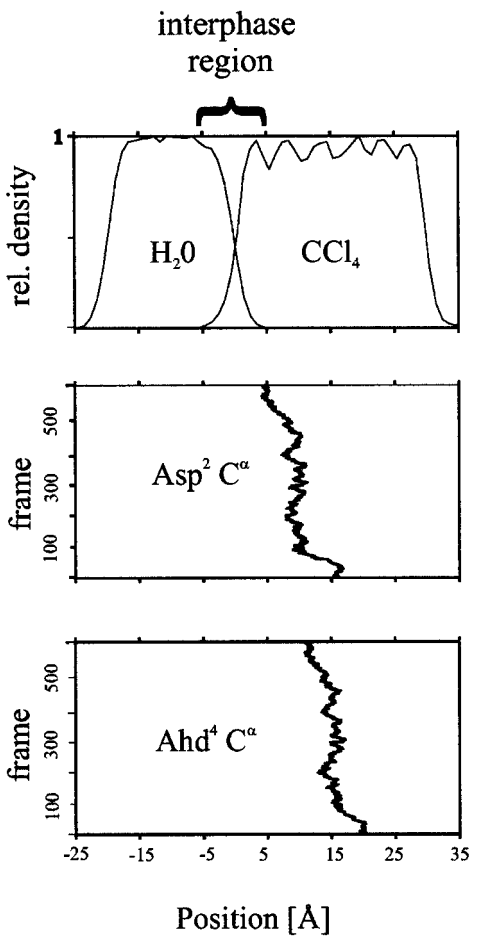

Figure 2 Interdigitation process of **C3** during the free simulation in the two-phase system, illustrated by the y-coordinates of Asp^2C^α and Ahd^4C^α. The Asp^2C^α inserts into the aqueous phase, whereas the Ahd^4C^α remains in the lipophilic CCl_4 phase.

DISCUSSION

The investigation of potential influences of the environment on the structure of a given compound always requires a fine-tuned balance between sufficiently rigid scaffolds, which allow the identification of the adopted structure, and structures which are flexible enough to permit solvent-induced conformational changes. Therefore, such investigations must represent a borderline walk between the two undesired cases, where either no structural changes can be detected, or where no defined structures are formed in any environment. As a consequence, the investigated compounds are often not rigid enough to allow a structure determination solely by means of NMR, and therefore computer-assisted calculations are indispensable. In addition, ideal undistorted structure elements, e.g. an ideal β-turn often found in cyclic hexapeptides can hardly be expected for the more flexible compounds.

The peptides **C4**, **C5** and **C6** belong to a structural class where no conformational changes could be observed in any of the used solvents. The compounds exhibit defined conformations without significant differences in isotropic and anisotropic solution.

No preferred conformation could be identified for **C1**, **C7** and **C8** neither in $CDCl_3$ nor in SDS/H_2O. Apparently, these peptides are very flexible and do not even allow the induction of a structure by a membrane-like environment.

For **C2**, neither DG nor SA calculations lead to a converging structure in $CDCl_3$. In micellar solution, however, at least a set of three structural families can be found, which might be indicative for a beginning structure induction caused by the anisotropic environment. Apparently, in micellar solution some structures are energetically favored.

The most interesting case was found for **C3**. For this peptide we clearly observed a conformational change induced by the switch from isotropic to anisotropic solution. In $CDCl_3$, the hexapeptide shows a β,β-turn motif with both glycines in the $i+1$ position of the turns, which is shifted by one position upon transition to micellar solution. **C3** differs from **C2** solely by the altered chirality of Asp[1]. We suspect, that the D-configurated amino acid introduces some rigidity into the molecule, which allows the population of a defined conformational state. The shifted β,β-motif places the lipophilic alkyl chains at the short side of the molecule and therefore one might suspect that this is due to a thereby facilitated penetration into the non-polar phase.

For **C3** in a biphasic mixture of polar and non-polar solvents one might expect an accumulation and orientation of the peptide at the interphase with the lipophilic tails of the aminohexadecanoic acids pointing into the non-polar phase, while the polar aspartic acids are oriented to the polar phase. Our membrane-mimicking CCl_4/H_2O system not only reproduced this obvious behavior, but also correctly reflected the conformational change, which was observed by separate calculations in $CDCl_3$ and the two-phase system. Therefore, the two-phase system appears to be a powerful tool for structure elucidation of membrane-active compounds, which might also help us to understand the contribution of membranes in the recognition process between ligand and receptor.

Taken together, we could demonstrate that anisotropic environments in certain cases are not only able to induce conformations in previously unstructured molecules, but may also induce conformational changes. However, it should be noted that the strongest influence of membranes on structural changes occurs when the membrane induces a change from previously non-amphiphilic molecules to amphiphilic structures.

Acknowledgements

Financial support by the Deutsche Forschungsgemeinschaft and the Fonds der Chemischen Industrie is gratefully acknowledged. M. Koppitz thanks the TU Munich for a fellowship. The authors thank Dr J. Winkler for contributing the FAB mass spectra.

REFERENCES

1. Deber, CM, Behnam, BA. *Proc. Natl. Acad. Sci. USA* 1984; **81**: 61–65.
2. Schwyzer, R. *Biochemistry* 1986; **25**: 4281–4286.
3. Schwyzer, R, Gremlich, HU, Gysin, B, Sargent, DF, Fringeli, HP. In *Peptides: Structure and Function*, Hruby, VJ, Rich, DH (eds), Illinois: Pierce Chemical Co., Rockford. 1983; 657–664.
4. Schwyzer, R. *Biochemistry* 1986; **25**: 6335–6342.
5. Liu, LP, Deber, CM. *Biochemistry* 1997; **36**: 5476–5482.
6. Li, SC, Kim, PK, Deber, CM. *Biopolymers* 1995; **35**: 667–675.
7. Taylor, JW. *Biochemistry* 1990; **29**: 5364–5373.
8. Taylor, JW. Ösapay, G. *Acc. Chem. Res.* 1990; **23**: 338–344.

9. Mihara, H, Kanmera, T, Yoshida, M, Lee, S, Aoyagi, H, Kato, T, Izumiya, N. *Bull. Chem. Soc. Jpn*. 1987; **60**: 697–706.
10. Kaiser, ET. *Trends Biochem. Sci*. 1987; **12**: 305–309.
11. Kaiser, ET, Kézdy, JF. *Proc. Natl. Acad. Sci. USA* 1983; **80**: 1137–1143.
12. Blanc, JP, Taylor, JW, Miller, RJ, Kaiser, ET. *J. Biol. Chem*. 1983; **258**: 8277–8284.
13. Caldwell, GA, Naider, F, Becker, JM. *Microbiol. Rev*. 1995; **59**: 406–422.
14. Bölker, M, Kahmann, R. *Plant Cell* 1993; **5**: 1461–1469.
15. Moon, S-S, Chen, JL, Moore, RE, Patterson, GML. *J. Org. Chem*. 1992; **57**: 1097–1103.
16. Branton, WD, Rudnick, MS, Zhou, Y. *Soc. Neurosci. Abstr*. 1992; **18**: 10.
17. Nutkins, JC, Mortshire-Smith, RJ, Packman, LC, Brodey, CL, Rainey, PB, Johnstone, K, Williams, DH. *J. Am. Chem. Soc*. 1991: **113**: 2621–2627.
18. v. Traber, R, Keller-Juslen, C, Loosli, H-R, Kuhn, M, v. Wartburg, A. *Helv. Chim. Acta* 1979; **62**: 1252.
19. Hart, KC, Donoghue, DJ. *Oncogene* 1997; **14**: 945–953.
20. Waterhous, DV, Johnson, WC. *Biochemistry* 1994; **33**: 2121–2128.
21. Naider, FR, Gounarides, J, Xue, C-B, Bargiota, E, Becker, JM. *Biopolymers* 1992; **32**: 335–339.
22. Stroup, AN, Rockwell, AL, Gierasch, LM. *Biopolymers* 1992; **32**: 1713–1725.
23. Bruch, MD, Rizo, J, Gierasch, LM. *Biopolymers* 1992; **32**: 1741–1754.
24. Xu, G-Y, Deber, CM. *Int. J. Pept. Protein Res*. 1991; **37**: 528–535.
25. Behling, RW, Jelinski, LW. *Biochem. Pharm*. 1990; **40**: 49–54.
26. Jelicks, LA, Broido, MS, Becker, JM, Naider, FR. *Biochemistry* 1989; **28**: 4233–4240.
27. Barlos, K, Chatzi, O, Gatos, D, Stavropoulos, G. *Int. J. Pept. Protein Res*. 1991; **37**: 513–520.
28. Barlos, K, Gatos, D, Kallistis, J, Papahotiu, G, Sotiriu, P, Wenqing, Y, Schäfer, W. *Tetrahedron Lett*. 1989; **30**: 3943–3946.
29. Brady, SF, Varda, SL, Freidinger, RM, Schwenk, DA, Mendlowski, M, Holly, FW, Veber, DF. *J. Org. Chem*. 1979; **44**: 3101–3105.
30. Shiori, T, Ninomiya, K, Yamada, S-I. *J. Am. Chem. Soc*. 1972; **90**: 6203–6205.
31. Still, WC, Kahn, M, Mitra, A. *J. Org. Chem*. 1978; **43**: 6.
32. Bax, A, Byrd, RA, Aszalos, A. *J. Am. Chem. Soc*. 1984; **106**: 7632–7633.
33. Braunschweiler, L, Ernst, RR. *J. Magn. Reson*. 1983; **53**: 521–528.
34. Jeener, J, Meier, BH, Bachmann, P, Ernst, RR. *J. Chem. Phys*. 1979; **71**: 4546–4553.
35. Kessler, H, Griesinger, C, Kerssebaum, R, Wagner, K, Ernst, R. R. *J. Am. Chem. Soc*. 1987; **109**: 607–609.
36. Bax, A, Davis, DG. *J. Magn. Reson*. 1985; **63**: 207–213.
37. Bothner-By, AA, Stephens, RL, Lee, J, Warren, DC, Jeanloz, RW. *J. Am. Chem. Soc*. 1984; **106**: 811–813.
38. Bax, A, Griffey, RH, Hawkins, LB. *J. Magn. Reson*. 1983; **55**: 301–315.
39. Müller, L. *J. Am. Chem. Soc*. 1979; **101**: 4481–4484.
40. Lerner, L, Bax, A. *J. Magn. Reson*. 1986; **69**: 375–380.
41. Kessler, H, Bermel, W, Griesinger, C. *6th Symposium of Magn. Resonanzspektroskopie*, 1985.
42. Bax, A, Sklenar, V, Clore, GM, Gronenborn, AM. *J. Am. Chem. Soc*. 1987; **109**: 6511–6513.
43. Neuhaus, D, Williamson, M. *The Nuclear Overhauser Effect in Structural and Conformational Analysis*, VCH Chemie: Weinheim, 1989.
44. Mierke, DF, Kessler, H. *Biopolymers* 1993; **33**: 1003–1017.
45. Havel, TF. *Prog. Biophys. Mol. Biol*. 1991; **56**: 43–78.
46. Havel, TF. DISGEO, Quantum Chemistry Exchange Program, Exchange No. 507, Indiana University, 1988.
47. Crippen, GM, Havel, TF. *Distance Geometry and Molecular Conformations*. Somerset, UK Research Studies Press LTD: Wiley, 1988.
48. Havel, TF, Wüthrich, K. *Bull. Math. Biol*. 1984; **46**: 673–698.
49. Havel, TF. *Biopolymers* 1990; **29**: 1565–1585.
50. Kirkpatrick, S, Gelatt Jr, CD, Vecchi, MP, *Science* 1983; **220**: 671–680.
51. Hagler, AT, Lifson, S, Dauber, P. *J. Am. Chem. Soc*. 1979; **101**: 5122–5130.
52. DISCOVER Version 3.0, BIOSYM Technologies, 10065 Barnes Canyon Road, CA 92121, USA.
53. Kessler, H. *Angew. Chem. Int. Ed. Engl*. 1982; **21**: 512–523.
54. Koppitz, M. *Diplomarbeit*, München, 1992.
55. Koppitz, M, Spellig, T, Kahmann, R, Kessler, H. *Int. J. Peptide Protein Res*. 1996; **48**: 377–390.
56. Toniolo, C, Crisma, M, Formaggio, F, Peggion, C, Monaco, V, Goulard, C, Rebuffat, S, Bodo, B. *J. Am. Chem. Soc*. 1996; **118**: 4952–4958.
57. Caldwell, GA, Wang, S-H, Xue, C-B, Jiang, Y, Lu, H-F, Naider, F, Becker, JM. *J. Biol. Chem*. 1994; **269**: 19817–19826.
58. Marcus, S, Caldwell, GA, Miller, D, Xue, CB, Naider, F, Becker, JM. *Mol. Cell. Biol*. 1991; **11**: 3603–3612.
59. Fujino, M, Kitada, C, Sakagami, Y, Isogai, A, Tamura, S, Suzuki, A. *Naturwissenschaften* 1980; **67**: 406–408.
60. Koppitz, M, Huenges, M, Gratias, R, Diefenbach, B, Jonzyk, F, Kessler, H. *Helv. Chim. Acta* 1997; **80**: 1280–1300.
61. McDonell, PA, Opella, SJ. *J. Magn. Reson. B* 1993; **102**: 120–126.
62. Takahashi, S. *Biochemistry* 1990; **29**: 6255–6264.
63. Brooks III, CL, Karplus, M, Pettitt, BM. *Proteins: A Theoretical Perspective of Dynamics, Structure and Thermodynamics, Advances in Chemical Physics, Vol. LXXI*. New York: Wiley, 1988.

64. Wider, G, Lee, KH, Wüthrich, KJ. Mol. Biol. 1981; **42**: 159–163.
65. Kallick, DA, Tessmer, MR, Wtts, CR, Li., C-Y. *J. Magn. Reson. B* 1995; **109**: 60–65.
66. van Buuren, AR, Berendsen, HJC. *Biopolymers* 1993; **33**: 1159–1166.
67. Ko, SY, Dalvit, C. *Int. J. Pept. Protein Res.* 1992; **40**: 380–382.
68. Kessler, H, Mierke, DF, Saulitis, J, Seip, S, Steuernagel, S, Wein, T, Will, M. *Biopolymers* 1992; **32**: 427–433.
69. Lautz, J, Kessler, H, van Gunsteren, WF, Weber, H-P, Wenger, RM. *Biopolymers* 1990; **29**: 1669–1687.
70. Kessler, H, Köck, M, Wein, T, Gehrke, M. *Helv. Chim. Acta* 1990; **73**: 1818–1832.
71. Kessler, H, Gehrke, M, Lautz, J, Köck, M, Seebach, D, Thaler, A. *Biochem. Pharmacol.* 1990; **40**: 169–173.
72. van Gunsteren, WF, Berendsen, HJC. *Angew. Chem.* 1990; **102**: 1020–1055.
73. Guba, W, Kessler, H. *J. Phys. Chem.* 1994; **98**: 23–27.
74. Guba, W, Haeßner, R, Breipohl, G, Henke, S, Knolle, J, Sanatgada, V, Kessler, H. *J. Am. Chem. Soc.* 1994; **116**: 7532–7540.
75. Moroder, L, Romano, R, Guba, W, Mierke, D. F, Kessler, H, Delporte, C, Winand, J, Christophe, J. *Biochemistry* 1993; **32**: 13551–13559.
76. Wagner, K. *Dissertation*, 1988.
77. Mierke, DF, Kurz, M, Kessler, H. *J. Am. Chem. Soc.* 1994; **116**: 1042–1049.
78. Kenmink, J, van Mierlo, CPM, Scheek, RM, Creighton, TE. *J. Mol. Biol.* 1993; **320**: 312–322.
79. Scheek, RM, Torda, AE, Kenmink, J, van Gunsteren, WF, *Computational Aspects of the Study of Biological Macromolecules by Nuclear Magnetic Resonance*. New York: Plenum Press, 1991; 209–217.
80. Weber, PL, Morrison, R, Hare, D. *J. Mol. Biol.* 1988; **204**: 483–487.
81. Kessler, H, Griesinger, C, Lautz, J, Müller, A, van Gunsteren, WF, Berendsen, HJC. *J. Am. Chem. Soc.* 1988; **110**: 3393–3396.
82. Matter, H, Kessler, H. *J. Am. Chem. Soc.* 1995; **117**: 3347–3359.

